

All-Optical Switching and Coupling Characteristics of Femtosecond Pulses in a Nonlinear Fiber Directional Coupler

その他（別言語等） のタイトル	非線形光ファイバカプラによるフェムト秒パルスの 全光スイッチング及び結合特性
著者	SHIGA Kazuya, NISHIKAWA Kyohei, ANDO Kazutoshi, IMAI Masaaki, IMAI Yoh
journal or publication title	Memoirs of the Muroran Institute of Technology
volume	54
page range	101-107
year	2004-11
URL	http://hdl.handle.net/10258/70

All-Optical Switching and Coupling Characteristics of Femtosecond Pulses in a Nonlinear Fiber Directional Coupler

Kazuya SHIGA*,Kyouhei NISHIKAWA**,Kazutoshi ANDOH***,Masaaki IMAI*,Yoh IMAI****

(Received 17 May 2004, Accepted 31 August 2004)

We analyze numerically the propagation of ultra-short optical pulses in a nonlinear fiber directional coupler by taking into account the dispersion effect of the coupling coefficient in nonlinear regimes. From split-step Fourier analysis of coupled nonlinear Schrödinger equations it is found that the pulse breakup occurs due to coupling coefficient dispersion. It is also demonstrated that the group velocity dispersion and its resultant pulse broadening dominate the switching behaviors of nonlinear directional coupler. To clarify the effect of intermodal dispersion, ultra-short optical pulses of 50 fs pulse duration from a mode-locked Ti:Sapphire laser are used. Comparing the experimental results with the numerical calculations, we can estimate the coupling coefficient dispersion provided that appropriate parameters are given for a nonlinear fused-tapered coupler.

Keywords: Nonlinear fiber directional coupler, Ultra-short optical pulses, All optical switching, Coupling coefficient dispersion, Coupled nonlinear Schrödinger equations

1 INTRODUCTION

Theory of nonlinear directional couplers (NLDCs) has been reported by Jensen early in 1980s⁽¹⁾. Since then, NLDCs have received much attention because of its possible application to all-optical switching and logic operations for use in ultra-high speed data processing and ultrafast communication systems. NLDCs have been realized so far by using a dual-core optical fiber coupler because it can work as an ultrafast all-optical switch (Ref(2), p295-301). The operation principle of NLDCs is based on optical Kerr effect in which the refractive index exhibits an

intensity-dependence. An ultrafast all-optical Kerr shutter⁽³⁾ and switching⁽⁴⁾ using NLDCs have also been proposed. The advantages of such a switching device are the ultrafast response time less than 10 fs and low pump power because of its high power-density and long interaction length. Integrated optical switching devices have also been considered for wavelength division multiplexing scheme⁽⁵⁾. However, the wavelength-dependent switching and coupling characteristics in the NLDC have not been reported thoroughly⁽⁶⁾.

The objective of this paper is to study an all-optical coupling and switching operation that is dependent on the wavelength of incident light in the NLDC. Coupled nonlinear Schrödinger equations which take into account the dispersion property of the coupling coefficient were analyzed numerically in the new coupled-mode formulation developed by K.S.Chiang and his coworkers⁽⁷⁾⁽⁹⁾. But, in their paper⁽⁹⁾ the propagation of short optical pulses has been analyzed by use of a Fourier series analysis method. As was

*Department of Electrical and Electronic Engineering

**Presently, Information-System Enterprises, Hitachi Cable,Ltd.

***Presently, Fiber-Optics Division, NTT Advanced Technology Corporation

****Department of Electrical and Electronic Engineering, Ibaraki University

pointed out later⁽¹⁰⁾, however, the results obtained when coupling coefficient dispersion was taken into account, i.e., $R' = C_1 L_D / T_0 \neq 0$, leads to the mirror inversion of those of the above paper in time domain. The discrepancy between these results comes from adopting an opposite form of the Fourier transform in the Fourier series analysis method. From such a circumstance, although a Fourier series analysis using the right Fourier transform is still applicable, we employed a modified version of the algorithm known as a split-step Fourier method to solve the nonlinear Schrödinger equation⁽¹¹⁾. The numerical calculations show that pulse breakup not only occurs but the pulse itself deforms due to coupling coefficient dispersion.

The experimental verification is carried out by using a mode-locked Ti:sapphire laser that produces approximately 50 fs pulses at wavelengths of 820-870 nm with a repetition rate of 81.7 MHz. The effect of intermodal dispersion in terms of coupling coefficient of a NLDC was then confirmed by comparison with the numerical results. It is the first time to our knowledge to demonstrate theoretically and experimentally how the coupling coefficient dispersion influences all-optical switching of femtosecond short optical pulses in a fused-tapered directional coupler, which was made in our laboratory.

2 COUPLED NONLINEAR Schrödinger EQUATIONS

Consider an evanescent-field coupler consisting of two identical single-mode optical fibers. It is known that such a directional coupler supports two normal modes: even and odd modes. The transfer of optical power in the coupler can be described by the beating between these two modes. When the optical power is high enough that the nonlinearity is important, optical power switching becomes dependent on the optical power. Though a silica fiber has weak Kerr nonlinearity, the use of a long evanescent-field coupler results in modification in the switching characteristics under high power input pulses. At the same time the long fiber coupler induces a large amount of intermodal dispersion⁽⁷⁾⁽⁸⁾. The width of optical pulse depends not only on the intermodal dispersion but also self-phase modulation (SPM), and then, limits the switching capacity of the nonlinear coupler. Such an incomplete switching gives rise to pulse distortion and pulse breakup.

The coupled nonlinear Schrödinger equations taking into account the first-order coupling coefficient dispersion are expressed as⁽¹¹⁾

$$i \left(\frac{\partial A_1}{\partial z} + \beta_1 \frac{\partial A_1}{\partial t} + \frac{\alpha}{2} A_1 + C_1 \frac{\partial A_2}{\partial t} \right) - \frac{\beta_2}{2} \frac{\partial^2 A_1}{\partial t^2} + \gamma |A_1|^2 A_1 + 2\gamma |A_2|^2 A_1 + C_0 A_2 = 0 \quad (1a)$$

$$i \left(\frac{\partial A_2}{\partial z} + \beta_1 \frac{\partial A_2}{\partial t} + \frac{\alpha}{2} A_2 + C_1 \frac{\partial A_1}{\partial t} \right) - \frac{\beta_2}{2} \frac{\partial^2 A_2}{\partial t^2} + \gamma |A_2|^2 A_2 + 2\gamma |A_1|^2 A_2 + C_0 A_1 = 0 \quad (1b)$$

A_1 and A_2 are the slowly varying amplitude of the guided mode in each the waveguide, $\beta_m = (d^m \beta / d\omega^m)_{\omega=\omega_0}$ where β is the propagation constant and ω is the angular frequency of incident light. β_2 is the group velocity dispersion, and α is the loss coefficient of the fiber waveguide. $\gamma = 2\pi n_2 / \lambda A_{\text{eff}}$ (n_2 the nonlinear refractive index, A_{eff} the effective core cross section) stands for the nonlinear coefficient, and λ is the wavelength of light. C_0 and C_1 are, respectively, the linear coupling coefficient and the first-order coupling coefficient dispersion which are defined by $C_m = (d^m C / d\omega^m)_{\omega=\omega_0}$ where $C = C(\omega)$ is the coupling coefficient in a directional coupler made of two single-mode fibers⁽⁷⁾ (or wave guides). It is noted that in eqs.(1a) and (1b) the effect of second-order coupling dispersion is neglected⁽¹¹⁾ so that we concentrate on the first-order coupling dispersion and the Kerr nonlinearities like SPM and XPM (cross-phase modulation) that affect the phase of coupled modes in a NLDC.

To solve the propagation equations for two guided modes, it is useful to employ a frame of reference moving with optical pulse at the group velocity $v_g = 1/\beta_1$ so that we introduce a time scale normalized to pulse width T_0 as $T = (t - z/v_g)/T_0 = (t - \beta_1 z)/T_0$ in eqs.(1a) and (1b). Also, it is convenient to introduce a normalized amplitude u by the definition $A(z, t) = P_0^{1/2} u(Z, T)$ and a normalized distance $Z = z/L_D = |\beta_2| z / T_0^2$ which is equivalent to a distance parameter normalized to the dispersion length $L_D = T_0^2 / |\beta_2|$ in terms of optical soliton in fiber⁽²⁾. Here, T_0 is the initial pulse width, and P_0 is the peak power of the fundamental soliton and is related to the soliton order $N = \gamma P_0 T_0^2 / |\beta_2|$. After substitution of these normalized parameters, eqs.(1a) and (1b) may be written as

$$i \left(\frac{\partial u_1}{\partial Z} + \frac{\alpha L_D}{2} u_1 + \frac{C_1 L_D}{T_0} \frac{\partial u_2}{\partial T} \right) - \frac{1}{2} \text{sgn}(\beta_2) \frac{\partial^2 u_1}{\partial T^2} + |u_1|^2 u_1 + 2|u_2|^2 u_1 + C_0 L_D u_2 = 0 \quad (2a)$$

$$i \left(\frac{\partial u_2}{\partial Z} + \frac{\alpha L_D}{2} u_2 + \frac{C_1 L_D}{T_0} \frac{\partial u_1}{\partial T} \right) - \frac{1}{2} \text{sgn}(\beta_2) \frac{\partial^2 u_2}{\partial T^2} + |u_2|^2 u_2 + 2|u_1|^2 u_2 + C_0 L_D u_1 = 0 \quad (2b)$$

where $\text{sgn}(\beta_2) = 1, -1$ holds for ordinarily and extraordinarily dispersion regime, respectively. In the

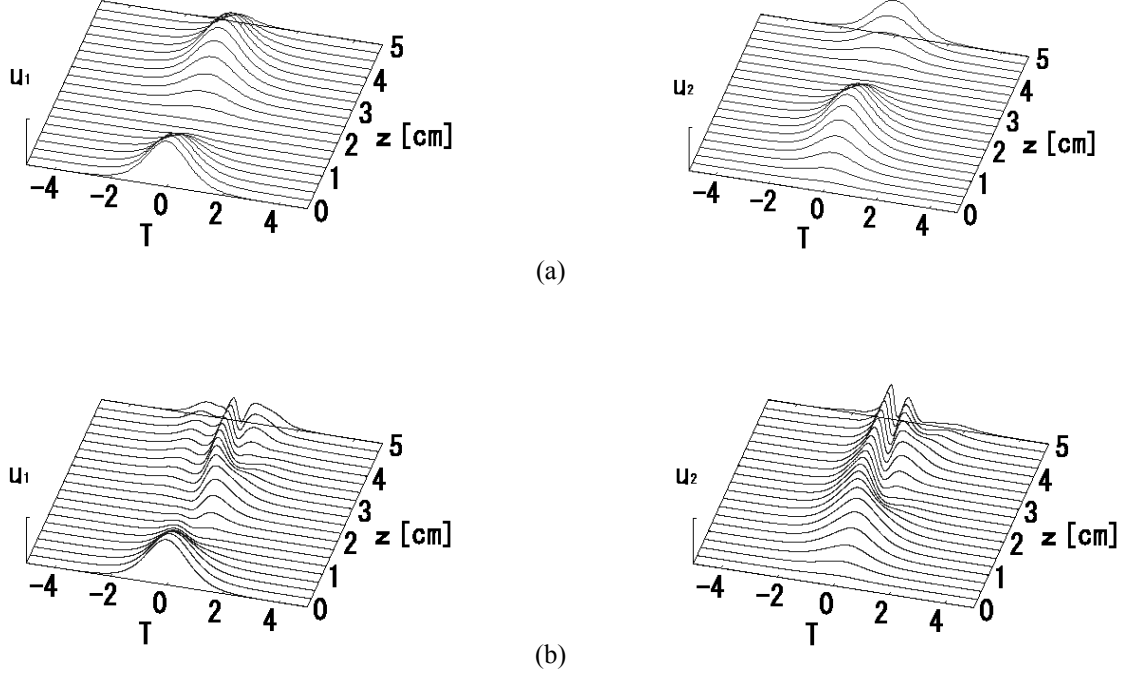


Fig.1 The pulse evolution in the nonlinear fiber coupler with $C_1=0$ in (a) and $C_1=-0.2$ ps/m in (b)

above equations, the coupling coefficient C_0 and the coupling coefficient dispersion C_1 are given by⁽⁷⁾

$$C_0 = \frac{(2\Delta)^{1/2} u^2}{av^3} \frac{K_0\left(\frac{wD}{a}\right)}{K_1^2(w)} \quad (3)$$

$$C_1 = \frac{(2\Delta)^{1/2} u^2}{\omega av^3} \frac{K_0\left(\frac{wD}{a}\right)}{K_1^2(w)} G \eta \quad (4)$$

where

$$G = \left[2 + 2w \frac{K_0(w)}{K_1(w)} - \frac{wD}{a} \frac{K_1\left(\frac{wD}{a}\right)}{K_0\left(\frac{wD}{a}\right)} \right] \times \left[1 + \frac{u^2}{w^2} \frac{K_0^2(w)}{K_1^2(w)} \right] - \left[1 + \frac{2K_0^2(w)}{K_1^2(w)} \right] \quad (5)$$

and

$$\eta = \frac{m_1 n_1 - m_2 n_2}{n_1^2 - n_2^2} \quad (6)$$

$$m_j = n_j + \omega \frac{dn_j}{d\omega} \quad (j=1,2) \quad (7)$$

where $j=1,2$ stand for the core and cladding, respectively, and $\Delta=(n_1-n_2)/n_1$, n_1 and n_2 the core and the cladding refractive index, a the core radius, D the separation between the cores. $u=ak(n_1^2-(\beta/k)^2)^{1/2}$ and $w=ak((\beta/k)^2-n_2^2)^{1/2}$ are the normalized transverse propagation constant and the normalized transverse attenuation constant, respectively, and $k=2\pi/\lambda$ the wavenumber in free space. Also, $v=(u^2+w^2)^{1/2} \approx akn_1(2\Delta)^{1/2}$ is the normalized frequency, and $K_{0,1}$ the modified Bessel functions of the first and second order, respectively.

Equation (2) is numerically evaluated by using a modified version of the split-step Fourier method¹¹⁾. The parameters used are set to be: 800 nm input optical wavelength ($\lambda_0=2\pi c/\omega_0$), 5.0 cm propagation distance (z), 100 fs input pulse duration (T_0), 3.3 μm core radius (a), 10.49 μm core separation (D), 89.77 m^{-1} for coupling coefficient (C_0), 39.26 ps^2/km for group velocity dispersion (β_2), 1.75 cm coupling length ($L_c=\pi/2C_0$), 2.97 normalized frequency (v). The incident pulse profile is assumed to be

$$\left. \begin{aligned} u_1(0, T) &= \text{sech}(T) \\ u_2(0, T) &= 0 \end{aligned} \right\} \quad (8)$$

where the normalized input peak power is assumed such that a peak value of $u_1(0, T)=1$ in eq.(8).

3 NUMERICAL RESULTS AND DISCUSSIONS

Numerical results of the pulse evolution in the nonlinear fiber coupler are shown in Fig. 1 in which the coupling coefficient dispersion $C_1=0$ in (a) and $C_1=-0.2$ ps/m in (b). For each case input peak power is assumed to be 20kW. When the coupling coefficient dispersion is ignored, the input pulse maintain its pulse shape as shown in (a). However, when taking account the coupling coefficient dispersion, the input pulse is divided into two peaks or more as well as the pulse profiles are distorted as shown in (b). The distortion in the pulse profile becomes remarkable when the propagation distance exceeds the coupling length (L_c). This property results in degradation in the switching characteristics of a NLDC and appears strongly as the input pulse becomes to be narrow. The dependence of power coupling on the input peak power is shown in Fig.2 in which the coupling coefficient dispersion $C_1=0$ and -0.09 ps/m. For the numerical calculations, the parameters of propagation distance $z=5$ cm, coupling coefficient $C_0=31.58\text{m}^{-1}$, coupling length $L_c=5$ cm are chosen in this case, whereas other parameters of T_0 , λ_0 and v are remained unchanged from those of Fig.1. When $P_0=0$ kW, the normalized output power of through port reduces to zero and complete power exchange occurs at $z=L_c$. This tendency is true for $C_1=0$ and -0.09 ps/m. In both the cases, the optical power at the through port is much greater than that of the cross port because of the nonlinear effect in the fiber. The output power does not exchange completely because the optical power in the leading and trailing edges in the pulse is not coupled due to small nonlinearity. At the wavelength of 800 nm, however, the effect of the so-called intermodal dispersion is not remarkable compared to those at longer wavelength, e.g., 1500 nm range that is longer than the zero-dispersion wavelength (1308 nm) and called the extraordinarily

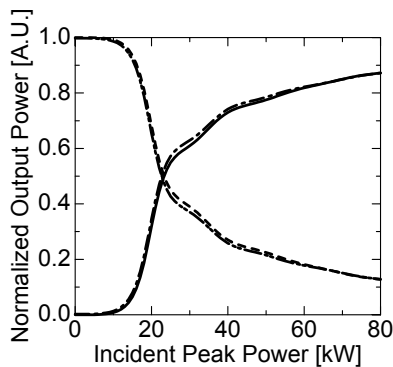


Fig.2 Dependence of power coupling on the incident peak power under the conditions of $C_1=0$ (— Through, - - - - Coupled) and $C_1=-0.09$ ps/m (— · — Through, · · · · Coupled)

dispersion regime⁽¹²⁾.

The dependence of power coupling on the wavelength of incident pulse is shown in Fig.3 in which $C_1=0$, $T_0=100$ fs in (a), $C_1=-0.2$ ps/m, $T_0=100$ fs in (b), and $C_1=-0.2$ ps/m, $T_0=50$ fs in (c). For each case of (a)-(c), the input peak power is assumed to be 10 kW, and other parameters of L_c at $\lambda_0=800$ nm and z are chosen as same in Fig.2. At the central wavelength of 800nm, an almost complete power exchange takes place since the condition of $z=L_c$ is satisfied.

When the coupling coefficient dispersion is ignored, the power exchange occurs completely in wide spectral range of wavelength as shown in (a). However, the coupling characteristics degrade in the longer wavelength region, when the coupling coefficient dispersion is taken into account, as shown in (b). This feature appears remarkably as the input pulse duration becomes short. The power does not exchange with each other in the longer wavelength region. The tendency of low-level power exchange is shown in (c). At the

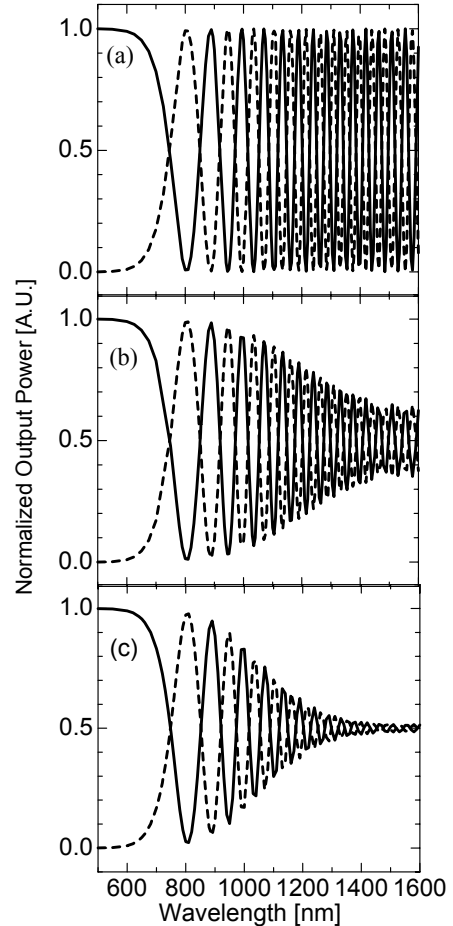


Fig.3 Dependence of power coupling on the wavelength under the conditions of $C_1=0$, $T_0=100$ fs, $P_0=10$ kW in (a), $C_1=-0.2$ ps/m, $T_0=100$ fs, $P_0=10$ kW in (b), $C_1=-0.2$ ps/m, $T_0=50$ fs, $P_0=10$ kW in (c) (— Through, - - - - Coupled)

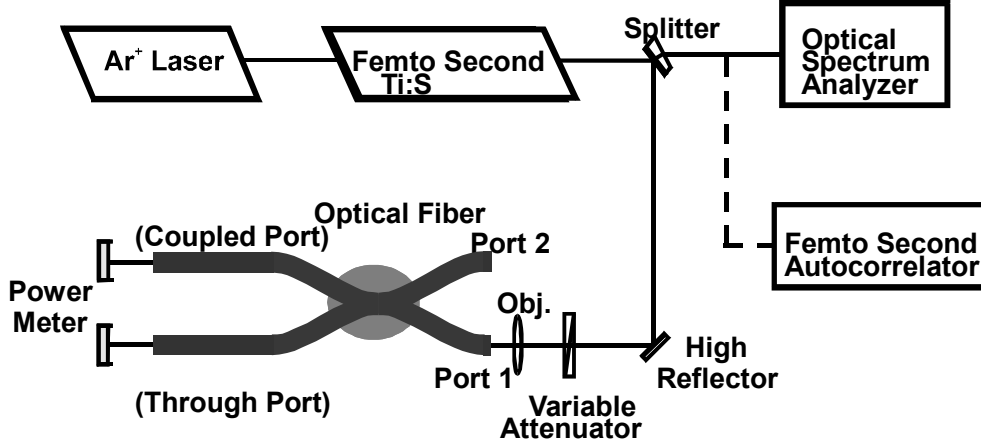


Fig.4 Experimental setup for measuring the power coupling of a NLDC

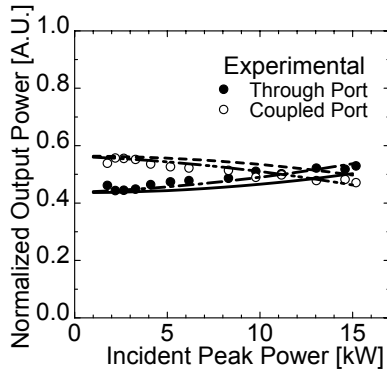

 Fig.5 Comparison of experimental power coupling dependent on incident peak power with the numerical results under the conditions of $C_1=0$ (— Through, - - - - Coupled) and $C_1=-0.16$ ps/m (- · - · Through, - - - - Coupled)

Table.1 The coupler parameters used for numerical analysis using a split-step Fourier analysis

Central wavelength λ_0	830 nm
Propagation distance z	4.52 cm
Incident pulse width T_0	100 fs
Core radius a	3.00 μm
Core separation D	10.12 μm
Coupling coefficient C_0	88.49 m^{-1}
Coupling coefficient dispersion C_1	0, -0.20 ps/m
Group velocity dispersion β_2	37.08 ps^2/km
Coupling length L_c	1.78 cm
Normalized frequency v	2.60

longer wavelength region, the pulse evolution is affected by the coupling coefficient more strongly than by the group velocity dispersion (β_2) because of the large coupling coefficient and then, the pulse separation occurs. This is the reason why power exchange does not take place in the longer wavelength region for a narrow input pulse.

4 EXPERIMENTAL VERIFICATION

Experimental setup for measuring the nonlinear coupling characteristics is shown in Fig. 4. A Kerr lens mode-locked femtosecond Ti:Sapphire laser pumped by Ar ion laser is used as a light source. The laser source produces optical pulses with 54 fs pulse width and 81.7 MHz repetition rate at 830 nm wavelength. The center wavelength of the emitted laser pulse is tuned over the range of 820-870 nm. The fused-tapered fiber coupler that is made in the institute's laboratory at Muroran IT is used for the nonlinear coupler. The whole length of the coupler is 46 cm which consists of a lead (front and rear) and a coupled section. The insertion loss is relatively as high as nearly 1 dB. The parameter of the fiber used for the coupler is as follows: 9.5 μm core diameter ($2a$), 1.308 μm zero-dispersion wavelength, 1.31 μm cut-off wavelength, 0.31 % relative index difference (Δ), 3.01×10^{-20} m^2/W for nonlinear refractive index (n_2). The NLDC parameters used for numerical analysis using a split-step Fourier method are listed in Table.1. As the preliminary experiment wide range wavelength-dependent coupling was measured by using a Halogen lamp with 50 W output power and 400-1700 nm spectrum width, instead of a Ti:Sapphire laser. The output from port 1 of the fiber coupler is detected and analyzed by an optical spectrum analyzer or a femtosecond autocorrelator. It is noted here that a femtosecond autocorrelator is used as a replacement of an optical spectrum analyzer and then, connected with a dotted line in Fig.4.

The coupling characteristics dependent on the incident peak power is shown in Fig. 5. In this case the wavelength and the duration of incident optical pulse are chosen as 830 nm and 100 fs, because at wavelengths shorter or longer than 830nm cross-coupling of through and coupled port powers does not occur fully at incident peak powers less than 10 kW within 800-850nm range, which has been clarified experimentally and numerically. The

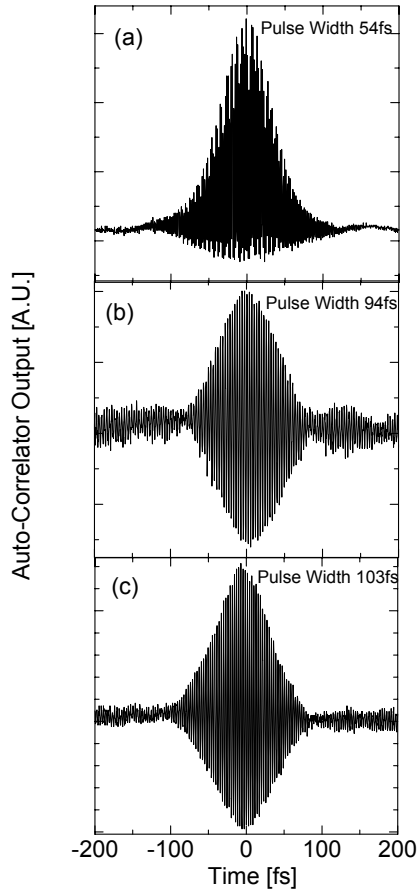


Fig.6 The auto-correlator outputs of the incident pulse (a) and the optical pulses at the through port (b) and the coupled port (c) of the NLDC

calculated results with and without intermodal dispersion are also shown with an appropriate line. It is obvious from Fig.5 that the experimental results are in good agreement with the numerical results taking into account the coupling coefficient dispersion, although a 100% switching characteristic has not been achieved so far. In order to obtain a higher switching power ratio, however, it is necessary to increase optical power coupled to a NLDC, as shown in Fig.2. As seen in Table.1, the fiber used the measurement is beyond the single-mode operation ($v=2.60$) at 830nm, but it is confirmed throughout the experiment that optical pulses from fs Ti:Sapphire laser are launched carefully into the center of a mirror leaved input end of fiber coupler. Therefore, the coupling into the dominant LP_{01} mode of the fiber may be satisfactory in a propagation through the fused-tapered coupler.

The incident and outgoing optical pulses are measured by an autocorrelator and shown in Fig. 6. The pulse duration was measured by a standard second-order autocorrelation method which is well known as a fringe resolved autocorrelation measurement developed by Diels et al^{(13),(14)}. The actual pulse duration (FWHM) was reduced to a scale ratio of 1/1.55, corresponding to sech^2 shaped pulses. The

incident pulse duration is 54 fs as shown in (a) and the output pulse width at the through and the coupled port are 94 fs and 103 fs, respectively, as shown in (b), (c). Therefore, it is confirmed that the pulse broadening occurs due to group velocity dispersion in the leading (front) part of fiber waveguide and intermodal dispersion of the coupling region discussed in Section 3. This is the reason why the parameter of $T_0=100\text{fs}$ is chosen instead of incident pulse duration $T_0=54\text{fs}$ in Table.1. It is also shown that the ratio of upper envelope and lower envelope of the auto-correlator outputs in (b) and (c) was different from that of input pulse in (a). For input pulse the autocorrelation ratio was found to be 8:1 whereas the output pulses of through and coupled ports possess the ratio of nearly 1:1. This is due to degradation of optical coherence of pulses since the ultra-short pulse is chirped by SPM⁽¹⁴⁾ (for example, by propagation through a Kerrlike nonlinearity in optical fiber).

From the results obtained it is confirmed that the pulse broadening occurs due to the intermodal dispersion in the coupling region as well as the group velocity dispersion at the input length of the fiber. It has been also pointed out that the variation of the input length of fiber preceding the tapered coupler has a dramatic effect on the spectral broadening of optical pulse⁽¹⁵⁾. From the comparison of numerical results and experiments of output power vs incident peak power shown in Fig.5, the coupling coefficient dispersion is estimated to be -0.16 ps/m. Irrespective of a small dispersive coupling effect, it should be noted that the pulse broadening due to intermodal dispersion degrades the performance of all-optical switching for a nonlinear fused-tapered coupler. Finally, it should be noted that the pulse breakup (twin peaks) shown in Fig.1 was not observed in the autocorrelator's output (triple peaks) because in Fig.5, the parameters fitted to the experimental are $\lambda_0=830\text{nm}$, $z=4.52\text{cm}$, and $L_c=1.78\text{cm}$, whereas $\lambda_0=800\text{nm}$, $z=5.0\text{cm}$, and $L_c=1.75\text{cm}$ were chosen in Fig.1. Even though such a discrepancy of these parameters influences the all-optical switching and coupling, the slightly deformed output in the trail of Fig.6(b) is likely due to the effect of coupling coefficient dispersion mentioned above.

5 CONCLUSIONS

The coupling characteristics of a nonlinear fiber coupler were investigated numerically and experimentally by using ultra-short optical pulses. It was confirmed that the pulse broadening occurs due to the intermodal dispersion combined with nonlinear optical effects and the group velocity dispersion. We also carried out experiments on NLDC using a mode-locked Ti:sapphire laser and compared with the theory. The experimental results of the power exchange were in good agreement with the numerical ones. As a conclusion, it is worthy to note that a dispersive

coupling coefficient could cause significant pulse distortion so that a nonlinear fused-tapered coupler may be used for switching of a short optical pulse with pulsewidth larger than 1ps. For such a pulse of $T_0 > 1ps$, it has been reported that the intermodal dispersion can be neglected at the wavelength of $1.55\mu m$ ⁽¹¹⁾. Thus, other effects such as higher-order dispersion and higher-order nonlinearities, i.e., stimulated Raman scattering and self-steepening, in addition to the effect of intermodal dispersion may lead to strong distortions for femtosecond pulses ($T_0 < 1ps$).

ACKNOWLEDGEMENTS

This research was supported in part by a grant-in-aid for scientific research from the Ministry of Education, Science and Culture, Japan under Grant No.13026202. The authors wish to thank Dr. Wataru Watanabe and Prof. Kazuyoshi Itoh, Osaka University, Graduate School of Engineering, for their kind assistance when performing the experiment with a mode-locked Ti:Sapphire laser at their laboratory and for useful discussion and comments to this work. As a final note, one (K.S.) of the authors is grateful to Prof. Shin Kagami, Muroran Institute of Technology for continuing encouragement and discussions on this work.

REFERENCES

- (1) S.M.Jensen, IEEE J.Quantum Electron, QE-18 (1982), p1580-1583.
- (2) G.P.Agrawal: *Nonlinear Fiber Optics*, (Academic Press, New York, 1995) 2nd ed., chap.7.
- (3) K.Kitayama, Y.Kimura, K.Okamoto and S.Seikai, Appl.Phys.Lett, 46 (1985), p623-625.
- (4) T.Morioka and M.Saruwatari, IEEE J.Select.Area Commun, 6 (1988), p1186-1198.
- (5) A.Villeneuve, C.C.Yang, P.G.J.Wigley, G.I.Stegeman, J.S.Aitchison and C.N.Ironside, Appl.Phys.Lett, 61 (1992), p147-149.
- (6) M.Imai, M.Kajinuma and J.Nakai, Tech.Dig.OECC'98 (The Institute of Electronics, Information and Communication Engineers, Tokyo, 1998), p294-295.
- (7) K.S.Chiang: Opt.Lett, 20 (1995), 997-999.
- (8) K.S.Chiang, J.Opt.Soc, Am.B 14 (1997), p1437-1443.
- (9) P.Shum, K.S.Chiang and W.A.Gambling, IEEE J.Quantum Electron, 35 (1999) 79.
- (10) X.Zhang, IEEE J.Quantum Electron, 37 (2001), p733-734.
- (11) P.M.Ramos and C.R.Paiva, IEEE J.Quantum Electron, 35 (1999), p983-989.
- (12) K.Andoh, K.Nishikawa, S.Sato and M.Imai, Tech. Report of IEICE, 2001-35 (2001), p43-48.
- (13) J.-C.Diels, E.W.VanStryland and D.Gold, "Picosecond Phenomena (eds. C.V.Shank, E.P.Ippen and S.L.Shapiro)", Springer-Verlag (1978), p.117-120.
- (14) J.-C.M.Diels, J.J.Fontaine, L.C.McMichael and F.Simoni, Appl. Opt., 24 (1985), p1270-1282.
- (15) P.Dumais, F.Gonthier, S.Lacroix, J.Bures, A.Villeneuve, P.G.J.Wigley and G.I.Stegeman, Opt.Lett, 18 (1993), p1996-1998.

非線形光ファイバカプラによるフェムト秒パルスの全光スイッチング及び結合特性

志賀 一哉*, 西川 恭平**, 安東 和俊***, 今井 正明*, 今井 洋****

概要

非線形領域における結合係数の分散効果を考慮した非線形ファイバカプラ中の超短光パルスの伝播の数値解析を行った。非線形シュレーディンガー方程式の SSF (split-step Fourier: スプリット ステップ フーリエ) 法による解析により、結合係数分散によりパルスの分離が起こることがわかる。それはまた、群速度分散及びその結果として生じるパルスの広がり非線形ファイバカプラのスイッチング動作で重要なことを示す。材料分散の効果を明らかにするため、モードロック Ti:サファイアレーザーからの 50[fs] のパルス幅の超短光パルスを用いて実験を行った。実験結果と数値計算を比較することで、非線形融着テーパ型光ファイバカプラの適切なパラメータが与えられた場合、結合係数分散を評価することができる。

キーワード: 非線形光ファイバカプラ、超短光パルス、全光スイッチング、結合係数分散、非線形結合シュレーディンガー方程式

*電気電子工学科、 **日立電線株式会社 情報システム事業本部、
 ***NTT アドバンステクノロジー株式会社 ファイバオプティクス事業部、
 ****茨城大学 電気電子工学科